

Reconstructing drought variability for Mongolia based on a large-scale tree ring network: 1520–1993

N. Davi,¹ G. Jacoby,^{1,2} K. Fang,³ J. Li,⁴ R. D'Arrigo,¹ N. Baatarbileg,^{1,2} and D. Robinson⁵

Received 21 January 2010; revised 18 August 2010; accepted 25 August 2010; published 16 November 2010.

[1] Previous tree ring based hydrologic studies in Mongolia have been regional in scale. Here, we present a large-scale summer drought reconstruction for Mongolia that reveals the main summer moisture patterns of the past. This reconstruction is based on a network of tree ring chronologies that span the country. The resulting drought model explains 61% of the variance and is extended to cover 1520–1993 by using a nested approach to modeling. Severe droughts and harsh winter conditions occurred in Mongolia from ~1999–2002 and contributed to massive livestock mortality and economic loss. These droughts were extreme in the context of the past several hundred years. Significant periodicities are found at 40 (90%), 19.3–25 (99%), 11.6 (95%), 6.4–7.2 (95%), and 2.8 years (99%). This high-resolution drought reconstruction and associated tree ring chronologies supplement and extend the sparse meteorological data in Mongolia and can be used to better understand climate variability and potential forcings of climate.

Citation: Davi, N., G. Jacoby, K. Fang, J. Li, R. D'Arrigo, N. Baatarbileg, and D. Robinson (2010), Reconstructing drought variability for Mongolia based on a large-scale tree ring network: 1520–1993, *J. Geophys. Res.*, 115, D22103, doi:10.1029/2010JD013907.

1. Introduction

[2] Evaluation of the instrumental record shows that Mongolia is undergoing significant climatic change [Yatagai and Yasunari, 1994; Batima et al., 2005; Endo et al., 2006]; this change includes pronounced warming, consistent with similar temperature increases elsewhere in the Northern Hemisphere and the globe. Warming has been particularly pronounced in the high mountain regions, such as the Altai Mountains (Figure 1) in the west [Batima et al., 2005]. Millennial length tree ring width records show that temperatures of the late 1990s to early 2000s were unprecedented in Mongolia [D'Arrigo et al., 2001]. How this warming will affect precipitation patterns in the future is difficult to predict [Christensen et al., 2007], as climate forcings in continental Asia and Mongolia are highly complex [Aizen et al., 2001].

[3] Precipitation variability in Mongolia is likely to result from a combination of various forcings, including the Siberian anticyclone circulation (in winter), the northward migration of the westerly jet stream (in summer), synoptic-

scale disturbances, continental evapotranspiration and evaporation from oceans, orography, and the Asian Monsoon [Aizen et al., 2001; Iwao and Takahashi, 2006]. There is only limited understanding of how these various factors impact climate in Mongolia, and much of midlatitude Asia. This is in part due to limited length and coverage of meteorological data in the region.

[4] For the above reasons, tree ring data have been used to create regional climate reconstructions that supplement and extend the limited meteorological record of Mongolia and can be used to help evaluate forcing influence through time. Scientists at the Tree-Ring Laboratory of Lamont-Doherty Earth Observatory, along with colleagues at the National University of Mongolia's Department of Forestry, have collected tree ring samples in Mongolia for the Mongolia-American Tree Ring Project (MATRIP) since 1995. These data include reconstructions of drought that reflect spatial and temporal patterns of moisture variability on interannual to centennial time scales [Pederson et al., 2001; Davi et al., 2006, 2009].

[5] Here we use an expanded network of tree ring records (34 sites) to create a larger-scale drought reconstruction of average June–August (JJA) Palmer Drought Severity Index (PDSI) for Mongolia (Figure 1). The PDSI is a widely used drought indicator based on a water balance model that considers water supply (precipitation), demand (evapotranspiration) and loss (runoff) [Palmer, 1965; Dai et al., 2004].

[6] In the Dai et al. [2004] study, the first principal component of an empirical orthogonal function (EOF) of global PDSI (1870–2002) shows global wetting and drying patterns. This EOF suggests a drying pattern over the majority of Mongolia. A subsequent analysis of PDSI over China and

¹Tree-Ring Laboratory, Lamont-Doherty Earth Observatory of Columbia University, Palisades, New York, USA.

²Tree-Ring Laboratory, Department of Forestry, National University of Mongolia, Ulaanbaatar, Mongolia.

³Key Laboratory of Western China's Environmental Systems, Lanzhou University, Lanzhou, China.

⁴International Pacific Research Center, School of Ocean and Earth Science and Technology, University of Hawai'i at Manoa, Honolulu, Hawaii, USA.

⁵Department of Geography, Rutgers, State University of New Jersey, Piscataway, New Jersey, USA.

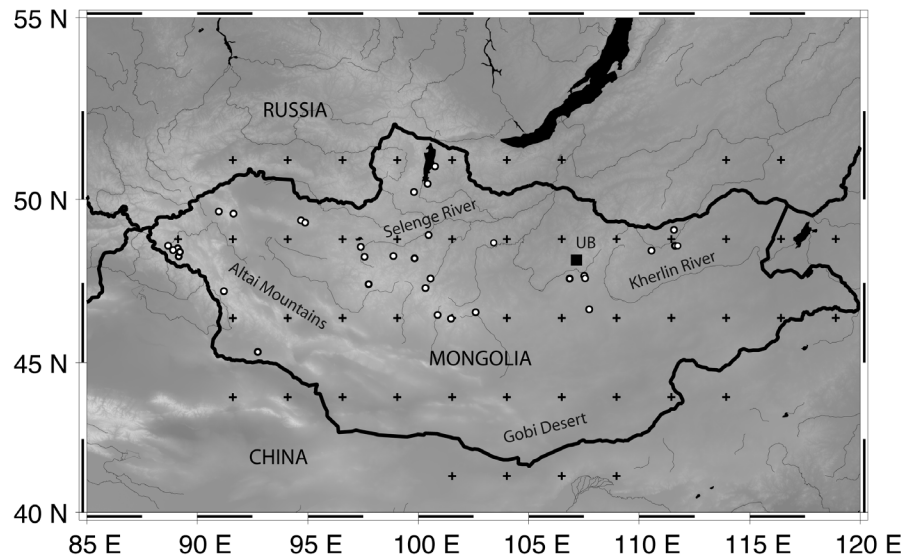


Figure 1. Map of study region showing the location of the 48 PDSI grid cells over Mongolia (crosses) and the locations of the 34 tree ring sites tested for modeling (white circles). The capital of Mongolia, Ulaan Baatar (UB), is shown as a square. Lighter shading indicates higher elevation.

Mongolia [Li *et al.*, 2009] found no significant moisture trend from 1951–2005 over central and western Mongolia. However, in eastern Mongolia there was an overall drying trend (statistically significant at the 0.01 level), particularly beginning in the early 1990s [Li *et al.*, 2009]. An average of all monthly PDSI over China and Mongolia (1951–2005) shows a decreasing trend beginning in the 1990s with 2001 being the driest year [Li *et al.*, 2009]. In Mongolia, a summer drought followed by harsh winter conditions (often referred to as dzud), occurred from 1999 to 2002 and again in 2004–2005 and resulted in large-scale livestock losses that devastated the nomadic herding population [Batima, 2006]. Another severe dzud also took place this past winter (2009–2010).

[7] The main goal of this study is to extend the drought history of Mongolia, a region where very little is known, by using a network of moisture-sensitive tree ring records to develop a PDSI reconstruction that reveals the main summer moisture patterns of the past. It is our intention to reconstruct drought recurrence from a temporal perspective in order to show large-scale properties of the variation such as trends, extremes and periodicities over the past nearly half millennium, allowing for a long-term perspective.

[8] This large-scale drought reconstruction can be used to better understand drought and dzud conditions historically and to inform agrarian and climate sustainability programs and can also be used to evaluate the possible effects of ocean/atmosphere climate events on precipitation patterns in Mongolia.

2. Material and Methods

2.1. Tree Ring Data and PDSI Data

[9] Thirty-four sites showed that they might contribute some information related to moisture availability, based on observations of site conditions and other factors and were evaluated for this study (Table 1). Of all the chronologies

used for modeling PDSI in this study, six were previously published in regional climate studies [Pederson *et al.*, 2001; Davi *et al.*, 2006, 2009].

[10] Conventional techniques of dendrochronology were employed in dating and chronology development [Cook and Kairiukstis, 1990]. All cores were marked with exact calendar dates and visually cross-dated by evaluating marker years (extremely narrow or wide rings). Cores were measured to the nearest 0.001 mm and checked for dating accuracy using COFECHA software [Holmes, 1983; Grissino-Mayer, 2001]. Series were standardized using conservative detrending methods (negative exponential and straight-line curve fits) and developed into chronologies using ARSTAN software [Cook, 1985]. We use the Standard version [Cook, 1985] of all chronologies for analysis as all the sites contained open canopy stands and the standard chronology is more appropriate than the ARS chronology for such sites [Cook, 1985].

[11] The common period for all chronologies is 1703–1994, beginning from 1403 to 1703 and ending from 1994 to 2004. Chronologies that began with fewer than six individual tree ring series were truncated to insure reliability of climate signal. Chronology strength through time was evaluated using the expressed population signal (EPS) and the running mean correlation coefficient (25 year window) between all tree ring series used in a chronology, or Rbar statistics. EPS is a measure of chronology reliability and evaluates the relationship between the sample size of a chronology and the common variance or signal within a chronology. All chronologies have an EPS of at least 0.80 [Wigley *et al.*, 1984] and an Rbar of at least 0.3.

[12] PDSI values generally range from +10 to –10, where wet years are positive and dry years are negative. Although Palmer [1965] would categorize severe drought or wet conditions as any values over –3 and +3, respectively, interpretations of the moisture severity of a given value depend on the local mean climate condition [Dai *et al.*, 2004]. In

Table 1. Site Chart^a

Site	Longitude (°E)	Latitude (°N)	Species	Full Period ^b	Average Intercorrelation	Number of Trees	Used in Regression
Ankhnyi Khoton	88.0	48.4	Larix sibirica	1584–2004	0.63	29	yes
Bairam Ger	90.6	49.6	Larix sibirica	1526–2005	0.67	17	yes
Bulgan Gol	90.6	47.1	Larix sibirica	1464–2004	0.46	25	no
Dadal	111.4	49.0	Larix sibirica	1665–2001	0.74	13	yes
Dalbai Valley	100.5	51.0	Larix sibirica	1642–2002	0.72	32	no
Dayan Nuur	88.5	48.2	Larix sibirica	1678–2005	0.67	11	yes
Hadagtai Uul	102.3	46.4	Larix sibirica	1601–1996	0.74	19	yes
Hovsgol Nuur	100.1	50.5	Larix sibirica	1627–1994	0.73	8	no
Ikh Khavvtag	92.2	45.0	Juniperus spp	1671–2005	0.52	33	yes
Inferno Ridge	111.4	48.5	Larix sibirica	1703–1996	0.79	18	yes
Kaizil Talbai	89.0	48.0	Larix sibirica	1640–2004	0.58	10	yes
Khorgo Lava	99.5	48.1	Larix sibirica	1490–2000	0.77	40	yes
Khar Uzuur	94.3	49.3	Larix sibirica	1671–1998	0.83	12	yes
Khovd Gol	88.5	48.4	Larix sibirica	1643–2004	0.63	13	yes
Khureegyin Oi	97.4	47.3	Larix sibirica	1594–1999	0.75	10	yes
Manzshir Hiid	106.6	47.5	L. sibirica P.sylvestris	1647–1994	0.83	8	yes
Mandal Hill	107.5	46.5	Larix sibirica	1622–2002	0.71	15	yes
Namyin Davaa Bayanhongor	101.2	46.2	Larix sibirica	1609–2001	0.71	13	yes
Onon gol	111.4	48.5	Larix sibirica	1665–2001	0.70	16	yes
Ovoont	91.3	49.5	Larix sibirica	1475–1999	0.79	19	yes
HPlar High Pass	98.6	48.2	Pinus siberica	1403–1994	0.52	8	yes
South Park Ridge	94.5	49.2	Larix sibirica	1476–1998	0.76	24	no
Sulchyin Medee	100.3	47.5	Larix sibirica	1616–2002	0.85	15	no
Suulyin Bagtraa	100.0	47.2	Larix sibirica	1454–1999	0.74	21	no
Telmen Beach	97.1	48.5	Larix sibirica	1649–1998	0.70	16	yes
Terelj	107.3	47.5	Larix sibirica	1647–2002	0.58	22	yes
Undur Ulaan	103.1	48.6	Larix sibirica	1547–2002	0.80	15	yes
Urgun Nars	110.3	48.3	Pinus sylvestris	1666–1996	0.83	16	yes
Khatran Hatgal	99.5	50.2	Larix sibirica	1610–2003	0.74	13	yes
Khoton Nuur	88.3	48.3	Larix sibirica	1508–2004	0.67	19	yes
Zuun Mod	107.3	47.5	Larix sibirica	1589–2001	0.87	26	yes
Zuun Mod Gol	97.2	48.2	Larix sibirica	1550–1998	0.65	18	no
Zuun Salaa Mod	100.2	48.8	Larix sibirica	1584–2001	0.80	20	yes
Zurkh Togol	100.6	46.3	Larix sibirica	1547–2002	0.60	19	yes

^aList of site names for all tree ring chronologies used in this study, as well as their locations, species, time spans, average series intercorrelation, and number of trees and regression model status.

^bFull period used that contains at least six samples.

Mongolia, mean annual precipitation is relatively low, accumulating roughly 100–200 mm in the dry south and 200–350 mm in mountainous regions [Sato and Kimura, 2006].

[13] Here, we use the average June–August (JJA) PDSI from 48 $2.5^\circ \times 2.5^\circ$ PDSI grid points across Mongolia (Figure 1). The Dai *et al.* [2004] PDSI data have been adjusted using a ‘Queens Case’ method, where any missing values are estimated by interpolating the eight neighboring grids [Elobaid *et al.*, 2009; E. Cook, personal communication, 2009]. The mean JJA PDSI for Mongolia is -0.81 (1951–2005) and shows extreme drying from 1999 to 2002 and again from 2004 to 2005 (hereafter, 2000 droughts). We truncated the Mongolian PDSI beginning in 1951 for this study due to the limited meteorological records before that time in this region.

2.2. PDSI Regression Model

[14] The PDSI tree ring model for Mongolia was created using principal component regression on the 1951–1993 common period. We validated using a split calibration verification scheme [Cook and Kairiukstis, 1990], that is, calibration (1972–1993) and verification (1951–1971), as well as calibration (1951–1971) and verification (1972–1993). Since tree growth can be influenced by climate conditions of both previous and current years, we included tree ring indices of

the previous and current year as candidate predictors in the reconstruction model.

[15] All standard tree ring chronologies and the PDSI data were prewhitened prior to regression analysis in order to maximize the common signal and minimize the amount of noise [Cook *et al.*, 1999]. The pooled autocorrelation (persistence) calculated through this process was added back into the PDSI reconstruction [Cook *et al.*, 1999] to generate an improved reconstruction model with low-frequency information.

[16] In order to develop a statistically reasonable reconstruction that fully utilized the longest chronologies, we used a nested model approach that was stepped back in 20 year increments [Cook *et al.*, 2002]. The reconstruction associated with each nest was rescaled (mean and variance) to match the most replicated model (1703–1993). In so doing, 10 nested reconstruction models were established, extending the model back 174 years past the common period (1703–1993) to 1520. The calibration/verification statistics and variance explained (R^2), for the model (and each amended nest), are shown in Table 2. Forward nests were tested using all chronologies that span to 2001 (Table 1).

[17] To evaluate the reconstruction for periodicities we perform a spectral analysis using multitaper method (MTM) of spectral analysis [Mann and Lees, 1996]. Spectral anal-

Table 2. Model Statistics^a

Period	Type	Statistic	1703	1680	1660	1640	1600	1580	1560	1540	1520	1500
1972–1993	calibration	r	0.81	0.82	0.77	0.71	0.73	0.74	0.74	0.72	0.76	0.76
1951–1971	verification	r	0.71	0.74	0.74	0.68	0.74	0.38	0.38	0.36	0.56	0.41
		RE	0.54	0.54	0.52	0.41	0.45	0.19	0.19	0.17	0.42	0.12
		CE	0.28	0.27	0.26	0.08	0.15	-0.27	-0.27	-0.3	0.09	-0.37
1951–1971	calibration	r	0.88	0.88	0.8	0.8	0.77	0.58	0.58	0.57	0.57	0.57
		r	0.74	0.74	0.72	0.63	0.68	0.58	0.58	0.58	0.58	0.58
1972–1993	verification	RE	0.28	0.28	0.33	0.23	0.31	0.27	0.27	0.33	0.33	0.33
		CE	0.01	0.01	0.08	-0.06	0.05	-0.01	-0.01	0.09	0.09	0.09
		number of predictors	33	32	25	19	14	6	6	4	3	
1951–1993	calibration	R2	0.61	0.6	0.55	0.49	0.48	0.42	0.42	0.39	0.45	

^aCalibration and verification statistics for nested model with 20 year intervals. Top four rows show calibration (1972–1993) and verification (1951–1971) periods, and fifth through eighth rows show results when these periods are reversed. RE is the reduction of error, and CE is coefficient of efficiency [Cook and Kairiukstis, 1990]; both are measures of shared variance between the actual and modeled series (values above zero indicate that the regression model has some skill). The bottom two rows show the number of predictors that load into the model using different nested intervals and the associated variance explained (R2).

ysis is a method for identifying periodicities within a time series and is often used to establish possible connections with forcing factors. We also compare the reconstruction to global sea surface temperature data [Rayner *et al.*, 2003; Kaplan *et al.*, 1998].

3. Results

3.1. PDSI Reconstruction

[18] Of the 34 chronologies tested for the most replicated nest (1703–1993) and 68 candidate predictors (years -1 and 1),

33 predictors were significantly correlated (0.1 level or higher) with the average JJA of 48 PDSI cells spanning the entire country of Mongolia. The first six principal components (PCs) of the 38 predictors, which cumulatively explain 65% of the total tree ring variance, were retained for use in regression. The resulting JJA PDSI model (Figure 2) explains 61% of the PDSI variance and demonstrates valid calibration/verification statistics (Table 2). As the model is extended further back in time with each subsequent nest (Figure 3, top), the number of predictors declines (Figure 3, bottom), as does the variance explained, due to a decrease in the number

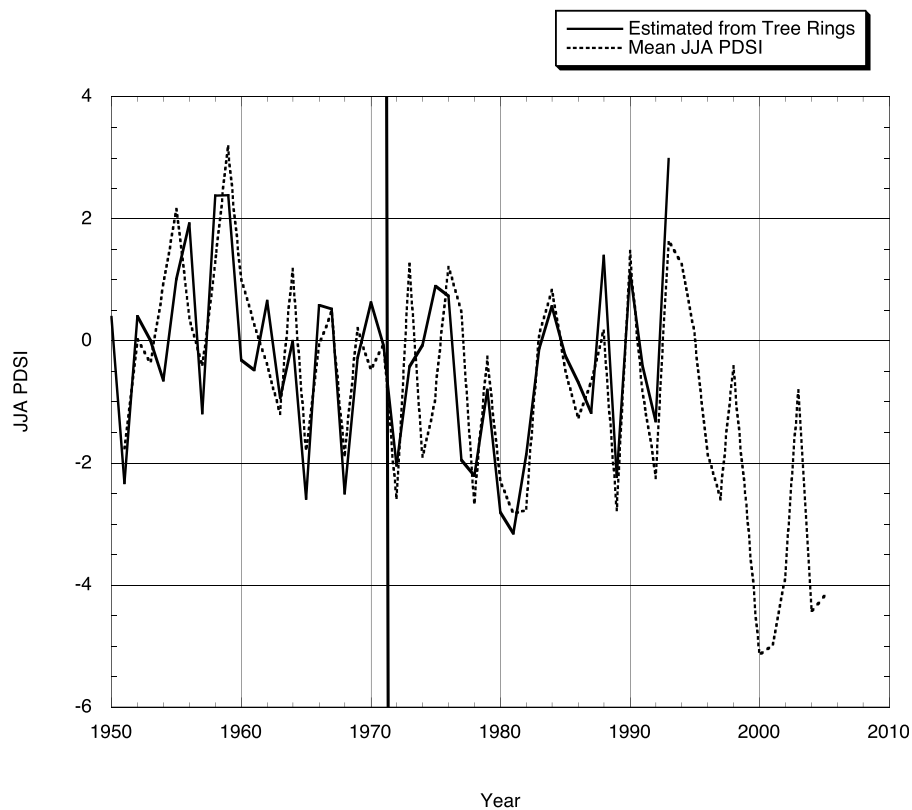


Figure 2. Comparison of actual (dotted line) and reconstructed (solid line) June–August PDSI averaged from 48 grid cells. Vertical line shows where the data are split for calibration and verification testing. $R = 0.78$ over the whole period (1951–1993). Note the extreme droughts from 1999 to 2003 and again from 2004 to 2005.

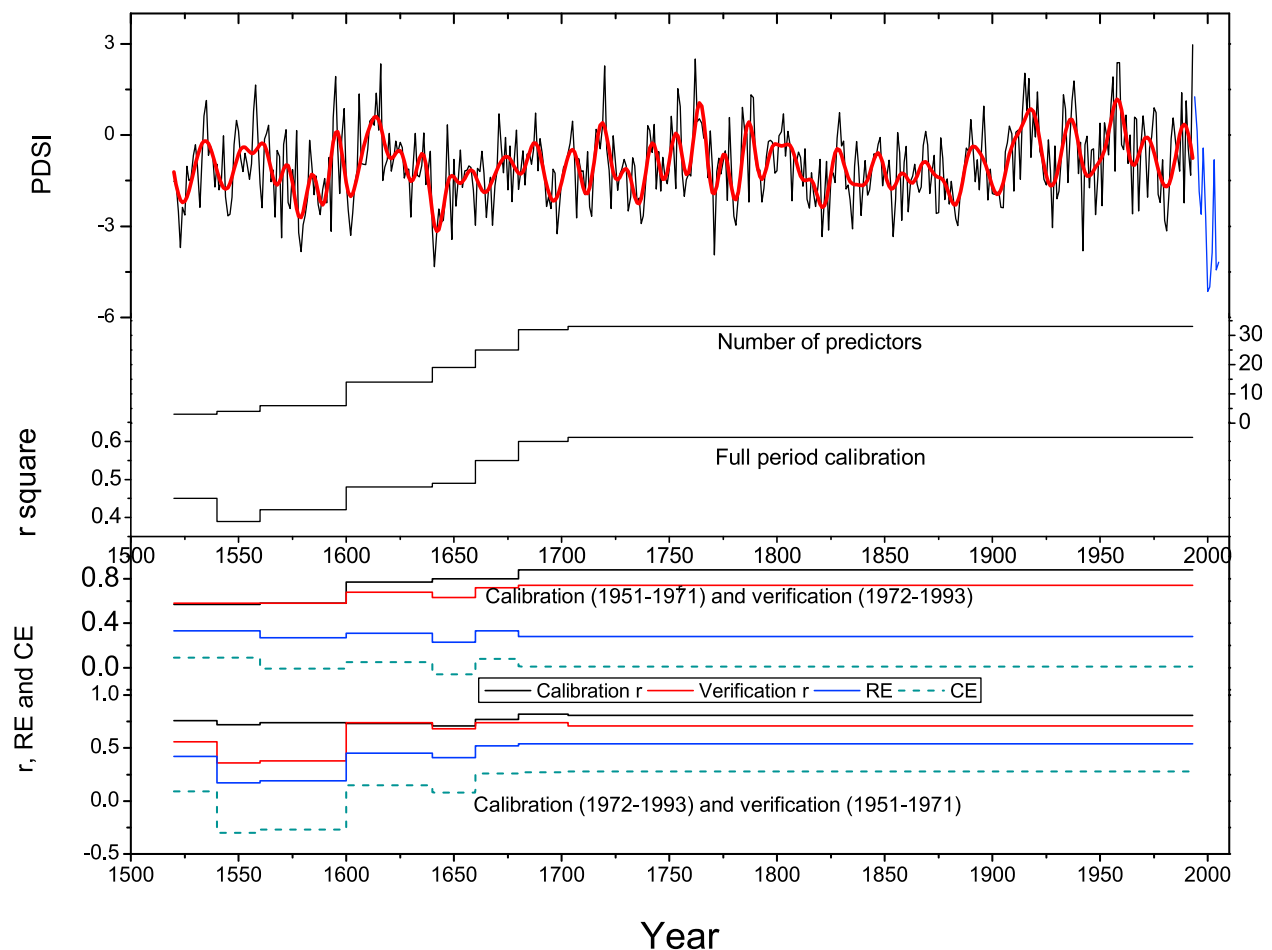


Figure 3. Summer (JJA) PDSI reconstruction based on tree rings (1520–1993) with the actual JJA PDSI values from 1994 to 2005 attached for context. The red line shows the data smoothed by using an adjacent-averaging method with an 11 year window. Also shown are the time-varying number of predictors, calibration r square for nested full period reconstruction, and the statistics of correlation (r), reduction of error (RE), and coefficient of efficiency (CE) for calibration and verification of the split periods (1951–1971 and 1972–1993).

of chronologies that cover the longer time span. Nests that were tested to extend the model past the year 1520 failed calibration and verification statistics and therefore were not included.

[19] A forward nest, using all tree ring chronologies that extend to 2001, was performed. Although the forward nest model captured the general year-to-year variation of the PDSI and correlated quite high ($R = 0.88$) we chose not to include it because the tree ring estimates underestimate the actual 1999–2000 PDSI values (Figure 4). The actual mean summer PDSI value for 2000 is -5.14 and estimates from tree rings are -1.87 (Figure 4). Mongolian tree ring chronologies that extend into 2001 (Table 1) and are located within the region that shows most extreme drought (auxiliary material Figure S1), have very narrow rings from 1999 to 2002.¹ This result demonstrates that the trees located in the driest regions during that time were in fact sensitive to these

droughts, although this effect is somewhat diluted in the large-scale average.

[20] A forward nest model (1994–2000) that includes tree rings that extend to 2001 and are located in the most drought-affected regions (auxiliary material Figure S1) captured the severity of the recent droughts more accurately than the large-scale average (actual PDSI value for 2000 is -5.14 , estimated from tree ring = -4.27) (Figure 4, red line) and shows that the 2000 droughts were severe in the context of the past several hundred years. However, because this drought is captured by a subset of tree ring chronologies we have decided not to include it in the PDSI model. Instead, we have included the actual average JJA PDSI data (of the 44 grid cells used for modeling) from 1994 to 2005 with the reconstruction in order to add context to the 2000 droughts (Figure 3).

3.2. Spectral Analysis

[21] The PDSI reconstruction (1703–1993) shows significant periodicities at 2.8 (99%), 6.4–7.2 (95%), 11.6 (95%), 19.3–25 (99%) and 40 years (90%) (Figure 5). All three

¹Auxiliary materials are available in the HTML. doi:10.1029/2010JD013907.

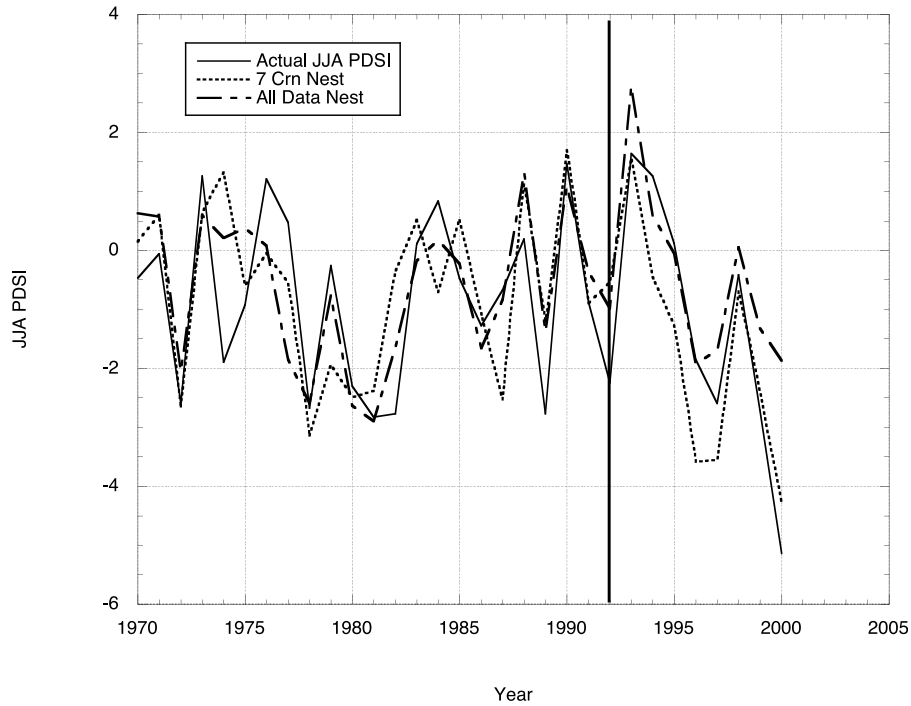


Figure 4. Graph showing the actual PDSI data (solid line), the forward nest using only chronologies from the most affected areas (dotted line), and the forward nest using all chronologies (dash-dotted line).

prior regional moisture reconstructions [Pederson *et al.*, 2001; Davi *et al.*, 2006, 2009] showed similar significant periodicities in the 6–7 year range, and 19–25 year range, although there was some overlap among the chronologies used in these various reconstructions (as six chronologies from previous work are incorporated into this study). Periodicities in the 11 and 22 year range are often seen in tree ring records [Rigozo *et al.*, 2003; Kasatkina *et al.*, 2006; Cook *et al.*, 1997]

and are thought to be associated with solar variability, although the climate mechanisms are not fully understood [Rind, 2002]. The 2–7 year periodicities are in the range of ENSO.

[22] A spectral analysis was also performed on the full nested reconstruction from 1520 to 1993, which shows similar periodicities as the most replicated period described above. These are in the interannual range at 2.9–3.0 (99%)

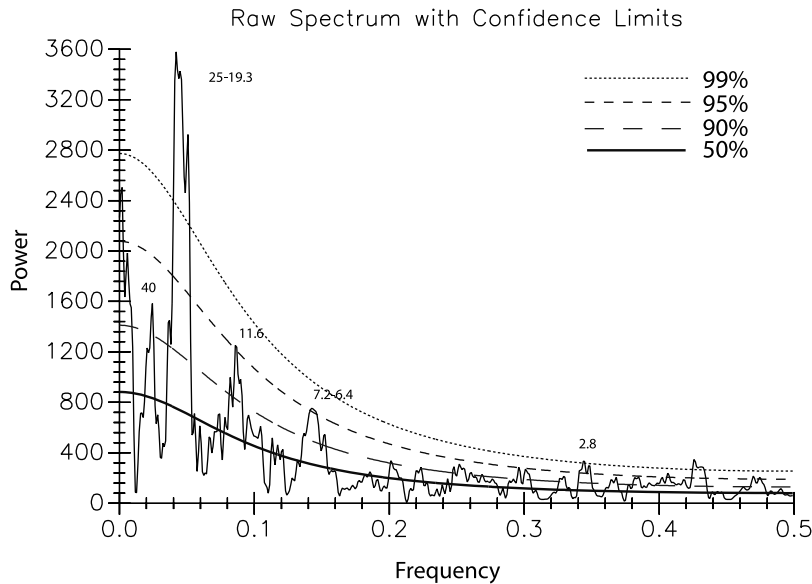


Figure 5. Plot of spectral properties of the most replicated JJA PDSI reconstruction (1703–1993) using multitaper method (MTM) spectral analysis [Mann and Lees, 1996]. Significant periodicities are marked with associated confidence limits: 99% (dotted line), 95% (short-dashed line), 90% (long-dashed line), and the null (solid line).

and 3.8 (99%) years and also in the decadal range at 19.6–22.7 years (99%). There is also a significant periodicity at 56 (95%) years.

3.3. Mongolian Drought and ENSO

[23] To further explore the significant periodicities in the 2–7 year range we compare the Mongolian drought reconstruction to ENSO-related sea surface temperature (SST) data [Smith and Reynolds, 2003]. We find that the Mongolian drought reconstruction is negatively correlated with average annual NINO3 (5°S to 5°N and 150°W to 90°W) ($R = -0.321$, $p = <0.05$ (detrended high-frequency correlations) over the 1951–1993 time interval, with lower correlations over the 1900–1993 interval ($R = -0.26$, $p = <0.05$).

[24] Spatial correlations of the all-Mongolia PDSI with SSTs (1951–1993) show that the negative correlations are located in the Niño region of the eastern equatorial Pacific. The correlation patterns are similar, but weaker, for the 1900–1993 period. The reconstruction also shows drought corresponding to years of known ‘super ENSOs’ in roughly 1789–1793 and 1982–1983. Very dry years are seen in the tree ring based forward nest during the major 1997–1998 El Niño event.

[25] Although there are limited diagnostic studies of the impacts of ENSO on Mongolian climate, much can be inferred from work on ENSO’s effect on precipitation in northern China [Zhang et al., 1999; Feng and Hu, 2004]. Feng and Hu [2004] find that northern China undergoes summer rainfall shortages when El Niño is in developing and maturing stages and relate variation in summer rainfall in northern China to ENSO by way of the Indian summer monsoon circulation (although the Indian monsoon is not part of ENSO per se). A possible mechanism for this connection is described by Zhang et al. [1999] and Feng and Hu [2004], who note a significant relationship between the northward flux of atmospheric moisture originating from the Indian Monsoon region and moisture convergence and rain in Northern China. We find correlation between the core India Monsoon precipitation [Parthasarathy et al., 1994] and the Mongolian drought reconstruction ($R = 0.50$ over the 1951–1993 period, and 0.36 over the 1900–1993 period) which supports these observations.

4. Discussion

4.1. Drought Forcings

[26] The time-varying nature of the apparent link to ENSO and lower correlations are not surprising given the distance to oceans and potential for influence by other forcings. Several studies [Iwao and Takahashi, 2006, 2008; Iwasaki and Nii, 2006] show that Rossby waves play a significant role in influencing summer precipitation variability in Mongolia. Iwao and Takahashi [2006, 2008] evaluated summer precipitation (~1950–2000) over NE Asia and identified a north-south seesaw mode between NE Asia and Siberia that forces precipitation change in Mongolia, particularly in June.

[27] The droughts (and harsh winter conditions) that occurred from 1999 to 2002 and again in 2004–2005 caused major livestock losses, were particularly severe in central Mongolia and follow some of the warmest summers seen in both instrumental temperatures and temperatures inferred

from tree rings for Mongolia [Batima et al., 2005; D’Arrigo et al., 2001]. These droughts were likely part of a much larger anomalous drought phenomenon that occurred across the midlatitudes of the northern hemisphere, spanning the United States, southern Europe and central and south Asia [Hoerling and Kumar, 2003; Barlow et al., 2002] during the winter and spring months. These hemispheric-scale droughts were linked to persistent La Niña conditions combined with anomalously warm SSTs in the western equatorial Pacific, which acted synergistically to form an anomalous zonal belt of high pressure spanning the midlatitudes [Hoerling and Kumar, 2003; National Weather Service Climate Prediction Center, 2002]. The record high temperatures further aggravated these droughts by increasing moisture demand [Hoerling and Kumar, 2003].

[28] The oceanic conditions that led to the 1999–2002 droughts were unusual because the warm SSTs were beyond what would be expected of natural variability and are linked, in part, to the oceans response to green house gases [Hoerling and Kumar, 2003], which suggests that continued warming, and warming in the western equatorial Pacific, could lead to increased frequency and severity of drought in Mongolia.

4.2. Spatial Complexities of Drought

[29] The summer droughts that took place in Mongolia from 1999 to 2002 show some regionality. Although much of the country was in extreme drought there are also regions that showed only mild drought and even some regions, such as the mountainous Altai, that were wetter than average. This spatial variability signifies that extreme regional droughts (or wet anomalies) can be masked by reconstructing an average PDSI for the entire country. Drought hazards for Mongolia may be even more severe (or less) on a regional basis than a country-wide reconstruction suggests and one must consider this when interpreting the all-Mongolia PDSI reconstruction developed here.

[30] For these recent droughts, it is also possible that the droughts were so severe in certain areas that those extreme indices dominate the countrywide average PDSI, effectively canceling out milder regions. The tree site locations, on the other hand, are spread over regions affected by a variety of moisture conditions during the 2000 droughts, resulting in country-wide estimates of drought (from trees) that are not as severe as the observed PDSI values. The fact that the most recent droughts are not fully reflected in the tree ring data across Mongolia demonstrates the influence of spatial variation and shows that one should not presume that drought is uniform. The trees capture the year-to-year variation of drought quite well during the rest of the regression period (1951–1993), however, the calibration period for the reconstruction is short and limited by the underlying station records, and must also be viewed as a limitation.

4.3. Other Drought Features

[31] An extreme multiyear drought also occurred from 1640 to 1646 (Table 3 and Figure 3). Evidence for drought conditions at this time was also found in a stalagmite record from Wanxiang Cave in central China [Zhang et al., 2008; Fang et al., 2009]. Although it is not clear if the 1640s droughts were one megadrought affecting much of central Asia, it is certainly a possibility. The summer drought of 2001 affected much of Mongolia, central and northeast

Table 3. Severe Drought: Driest 1 and 5 Year Periods

Rank	Dry Year	Dry 5 Year	Wet Year	Wet 5 Year
1	2000 ^a	2000–2004 ^a	1993	1955–1959
2	2001 ^a	1600–1644	1762	1612–1616
3	2004 ^a	1578–1582	1959	1915–1919
4	1641	1521–1525	1958	1762–1766
5	2005 ^a	1880–1884	1616	1990–1994
6	1771	1600–1604	1720	1916–1920
7	2002 ^a	1735–1739	1915	1716–1720
8	1579	1977–1981	1595	1934–1938
9	1942	1821–1825	1956	1751–1755
10	1523	1779–1783	1917	1785–1789

^aData from 1994 to 2005 are from averaged JJA PDSI.

China, Myanmar and northern Thailand. Similar spatial drought patterns are seen in 1999, 2000 and 2002. Other multiyear and single dry and wet years are listed in Table 3.

[32] An overall decrease in moisture variability in Mongolia is seen in the 1800s. This pattern was first identified by Pederson *et al.* [2001], who presented a tree ring based reconstruction for both streamflow and precipitation based on two chronologies (which have also been included in this study). Two of the driest 5 year periods for Mongolia occur during this century, from 1821 to 1825 and again from 1880 to 1884 (Table 3). The 1900s and beginning of the 20th century show more variability with extremely wet periods from 1915 to 1919, 1934–1938, 1955–1959, 1990–1994 and extremely dry years in 1928, 1942, 1977–1981 and again from 1999 to 2001 and 2004–2005 (Figure 3).

5. Summary and Conclusions

[33] We have described a nearly 500 year nested summer drought reconstruction for Mongolia based on a large-scale network of tree ring chronologies. This reconstruction provides a long-term context for spatially averaged drought conditions for Mongolia. Extremely dry periods, listed in decreasing order of severity, are reconstructed for 1600–1644, 1578–1582, 1880–1884, 1600–1604, 1735–1739, 1977–1981, 1821–1825, and 1779–1783.

[34] Spectral analysis shows significant periodicities at 2.8 (99%), 6.4–7.2 (95%), 11.6 (95%), 19.3–25 (99%) and 40 years (90%). Periodicities in the 11 and 22 year range are often found in tree ring records and are often associated with solar variability. Two to seven year periodicities are within the ENSO range. The Mongolia PDSI reconstruction is negatively correlated to ENSO, meaning that during ENSO events drier conditions tend to occur over Mongolia. An association between ENSO departures and Mongolia drought is also seen in spatial correlation maps of SST data. More research is needed to better understand the dynamics of oceanic and atmospheric conditions that force drought and moisture variability in Mongolia.

[35] Given the frequency and severity of drought and dzud conditions over this past decade, a more complete understanding of past climate variability and potential climate forcings is imperative for suitable risk management strategies. Currently, predictions of precipitation for Mongolia are uncertain during the summer, when most of the precipitation falls [Christensen *et al.*, 2007]. Synoptic-scale studies have been limited in Mongolia, in part due to the lack of meteorological records and the complexity of climatic conditions

in the region, and the effects and feedbacks of many possible forcings are difficult to delineate.

[36] We have presented a long-term perspective of spatially averaged drought variability for Mongolia spanning nearly 500 years. The tree ring network described herein, used in conjunction with available meteorological data, provides another significant step toward a better understanding of climate variability and forcings in the region.

[37] **Acknowledgments.** This research was supported by the National Science Foundation under grants ATM0117442 and OCE0402474. Special thanks go to Neil Pederson, Brendan Buckley, Byambagerel Suran, Oyunsanna Byambasuren, Uyanga Ariya, Biligbaatar Nanzad, Paul Krusic, Ed Cook, Erika Mashig, Francesco Fiondella, Ashley Curtis, Allyson Carroll, Tony Broccoli, Laura Schneider, and several anonymous reviewers. Lamont-Doherty Earth Observatory publication 7391.

References

- Aizen, E., V. Aizen, J. Melack, T. Nakamura, and T. Ohta (2001), Precipitation and atmospheric circulation patterns at mid-latitudes of Asia, *Int. J. Climatol.*, *21*, 535–556, doi:10.1002/joc.626.
- Barlow, M., H. Cullen, and B. Lyon (2002), Drought in central and southwest Asia: La Niña, the warm pool and Indian Ocean precipitation, *J. Clim.*, *15*, 697–700, doi:10.1175/1520-0442(2002)015<0697:DICASA>2.0.CO;2.
- Batima, P. (2006), Potential impacts of climate change and vulnerability and adaptation assessment for grassland ecosystem and livestock sector in Mongolia, *Final Rep.*, *303*, 105 pp., AIACC, Washington, D. C.
- Batima, P., L. Natsagdorj, P. Gombluudev, and B. Erdenetssetseg (2005), Observed climate change in Mongolia, *Working Pap.*, *12*, AIACC, Washington, D. C.
- Christensen, J. H., et al. (2007), Regional climate projections, in *Climate Change 2007: The Physical Science Basis, Contribution of Working Group I to the Fourth Assessment Report of the Intergovernmental Panel on Climate Change*, edited by S. Solomon et al., pp. 849–940, Cambridge Univ. Press, Cambridge, U. K.
- Cook, E. R. (1985), A time series analysis approach to tree-ring standardization, Ph.D. dissertation, 171 pp., Univ. of Ariz., Tucson.
- Cook, E. R., and L. A. Kairiukstis (1990), *Methods of Dendrochronology: Applications in the Environmental Sciences*, Kluwer, Dordrecht, Netherlands.
- Cook, E. R., D. M. Meko, and C. W. Stockton (1997), A new assessment of possible solar and lunar forcing of the bidecadal drought Rhythm in the western United States, *J. Clim.*, *10*, 1343–1356, doi:10.1175/1520-0442(1997)010<1343:ANAOPS>2.0.CO;2.
- Cook, E. R., D. M. Meko, D. Stahle, and M. K. Cleveland (1999), Drought reconstructions for the continental United States, *J. Clim.*, *12*, 1145–1162, doi:10.1175/1520-0442(1999)012<1145:DRFTCU>2.0.CO;2.
- Cook, E. R., R. D'Arrigo, and M. Mann (2002), A well-verified, multi-proxy reconstruction of the winter North Atlantic Oscillation index since AD 1400, *J. Clim.*, *15*, 1754–1764, doi:10.1175/1520-0442(2002)015<1754:AWVMRO>2.0.CO;2.
- Dai, A., K. E. Trenberth, and T. Qian (2004), A global data set of Palmer Drought Severity Index for 1870–2002: Relationship with soil moisture and effects of surface warming, *J. Hydrometeorol.*, *5*, 1117–1130, doi:10.1175/JHM-386.1.
- D'Arrigo, R., G. Jacoby, D. Frank, N. Pederson, B. Buckley, B. Nachin, R. Mijiddorj, and C. Dugarjav (2001), 1738 years of Mongolian temperature variability inferred from a tree-ring width chronology of Siberian pine, *Geophys. Res. Lett.*, *28*, 543–554, doi:10.1029/2000GL011845.
- Davi, N. K., G. C. Jacoby, A. E. Curtis, and B. Nachin (2006), Extension of drought records for central Asia using tree rings: West central Mongolia, *J. Clim.*, *19*, 288–299, doi:10.1175/JCLI3621.1.
- Davi, N., G. Jacoby, R. D'Arrigo, N. Baatarbileg, J. Li, and A. Curtis (2009), A tree-ring based drought index reconstruction for far western Mongolia: 1565–2004, *Int. J. Climatol.*, *29*, 1508–1514, doi:10.1002/joc.1798.
- Elobaid, R., M. Shitan, N. A. Ibrahim, A. N. A. Ghani, and I. Daud (2009), Evolution of spatial correlation of mean diameter: A case study of trees in natural dipterocarp forest, *J. Math. Stat.*, *5*(4), 267–269, doi:10.3844/jmssp.2009.267.269.
- Endo, N., T. Kadota, J. Matsumoto, B. Ailikun, and T. Yasunari (2006), Climatology and trends in summer precipitation characteristics in Mongolia for the period 1960–1998, *J. Meteorol. Soc. Jpn.*, *84*(3), 543–551, doi:10.2151/jmsj.84.543.

- Fang, K., N. Davi, X. Gou, F. Chen, E. Cook, J. Li, and R. D'Arrigo (2009), Spatial drought reconstruction for central high Asia based on tree rings, *Clim. Dyn.*, *4*, 277–288, doi:10.1007/s00382-009-0739-9.
- Feng, S., and Q. Hu (2004), Variations in the teleconnection of ENSO and summer rainfall in northern China: A role of the Indian summer monsoon, *J. Clim.*, *17*, 4871–4881, doi:10.1175/JCLI-3245.1.
- Grissino-Mayer, H. (2001), Evaluating crossdating accuracy: A manual and tutorial for the computer program COFECHA, *Tree Ring Res.*, *57*(2), 205–221.
- Hoerling, M., and A. Kumar (2003), The perfect ocean for drought, *Science*, *299*, 691–694, doi:10.1126/science.1079053.
- Holmes, R. L. (1983), Computer-assisted quality control in tree-ring dating and measurement, *Tree Ring Bull.*, *44*, 69–75.
- Iwao, K., and M. Takahashi (2006), Interannual change in summertime precipitation over northeast Asia, *Geophys. Res. Lett.*, *33*, L16703, doi:10.1029/2006GL027119.
- Iwao, K., and M. Takahashi (2008), A precipitation seesaw mode between northeast Asia and Siberia in summer caused by Rossby waves over the Eurasian continent, *J. Clim.*, *21*, 2401–2419, doi:10.1175/2007JCLI1949.1.
- Iwasaki, H., and T. Nii (2006), Mongolian rainy season and its relation to the stationary Rossby wave along the Asian Jet, *J. Clim.*, *19*, 3394–3405, doi:10.1175/JCLI3806.1.
- Kaplan, A., M. Cane, Y. Kushnir, A. Clement, M. Blumenthal, and B. Rajagopalan (1998), Analyses of global sea surface temperature 1856–1991, *J. Geophys. Res.*, *103*(18), 567–589.
- Kasatkina, E., O. Shumilov, N. V. Lunina, M. Krapiec, and G. Jacoby (2006), Stardust component in tree rings, *Dendrochronologia*, *24*(2–3), 131–135.
- Li, J., E. Cook, R. D'Arrigo, F. Chen, and X. Gou (2009), Moisture variability across China and Mongolia, *Clim. Dyn.*, *32*, 1173–1186, doi:10.1007/s00382-008-0436-0.
- Mann, M., and J. Lees (1996), Robust estimation of background noise and signal detection in climatic time series, *Clim. Change*, *33*, 409–445, doi:10.1007/BF00142586.
- National Weather Service Climate Prediction Center (2002), Expert assessments/climate assessments: Yangtze River flooding: July–August 2002, report, Camp Springs, Md. (Available at http://www.cpc.noaa.gov/products/expert_assessment/china2002/china_mongolia.shtml)
- Palmer, W. C. (1965), Meteorological drought, *Res. Pap.*, *45*, U.S. Dept. of Commer. Weather Bur., Washington, D. C.
- Parthasarathy, B., A. A. Munot, and D. R. Kothawale (1994), All India monthly and seasonal rainfall series: 1871–1993, *Theor. Appl. Climatol.*, *49*, 217–224, doi:10.1007/BF00867461.
- Pederson, N., G. Jacoby, R. D'Arrigo, E. Cook, B. Buckley, C. Dugarjav, and R. Mijiddorj (2001), Hydrometeorological reconstructions for northeastern Mongolia derived from tree rings: AD 1651–1995, *J. Clim.*, *14*(5), 872–881, doi:10.1175/1520-0442(2001)014<0872:HRFNMD>2.0.CO;2.
- Rayner, N. A., D. E. Parker, E. B. Horton, C. K. Folland, L. V. Alexander, D. P. Rowell, E. C. Kent, and A. Kaplan (2003), Global analyses of sea surface temperature, sea ice, and night marine air temperature since the late nineteenth century, *J. Geophys. Res.*, *108*(D14), 4407, doi:10.1029/2002JD002670.
- Rigozo, N. R., L. E. A. Vieira, E. Echer, and D. J. R. Nordemann (2003), Wavelet analysis of solar-ENSO imprints in tree ring data from southern Brazil in the last century, *Clim. Change*, *60*, 329–340, doi:10.1023/A:1026048124353.
- Rind, D. (2002), The Sun's role in climate variations, *Science*, *296*, 673–677, doi:10.1126/science.1069562.
- Sato, T., and F. Kimura (2006), Regional climate simulations to diagnose environmental changes in Mongolia, *Bull. Terr. Environ. Res. Cent.*, *7*, 59–69.
- Smith, T. M., and R. W. Reynolds (2003), Extended reconstruction of global sea surface temperatures based on COADS data (1854–1997), *J. Clim.*, *16*, 1495–1510.
- Wigley, T. M. L., K. R. Briffa, and P. D. Jones (1984), On the average value of correlated time series, with applications in dendroclimatology and hydrometeorology, *J. Appl. Meteorol.*, *23*, 201–213, doi:10.1175/1520-0450(1984)023<0201:OTAVOC>2.0.CO;2.
- Yatagai, A., and T. Yasunari (1994), Trends and decadal-scale fluctuations of surface air temperature and precipitation over China and Mongolia during the recent forty-year period (1951–1990), *J. Meteorol. Soc. Jpn.*, *72*, 937–957.
- Zhang, P., et al. (2008), A test of climate, Sun and culture relationships from an 1810-yr Chinese cave record, *Science*, *322*, 940–942, doi:10.1126/science.1163965.
- Zhang, R., A. Sumi, and M. Kimoto (1999), A diagnostic study of the impact of El Niño on the precipitation in China, *Adv. Atmos. Sci.*, *16*(2), 229–241.

N. Baatarbileg, Tree-Ring Laboratory, Department of Forestry, National University of Mongolia, Ulaanbaatar 210646, Mongolia.

R. D'Arrigo, N. Davi, and G. Jacoby, Tree-Ring Laboratory, Lamont-Doherty Earth Observatory of Columbia University, Palisades, NY 10964, USA. (ndavi@Ldeo.columbia.edu)

K. Fang, Key Laboratory of Western China's Environmental Systems, Lanzhou University, Lanzhou 730000, China.

J. Li, International Pacific Research Center School of Ocean and Earth Science and Technology, University of Hawai'i at Manoa, Honolulu, HI 96822, USA.

D. Robinson, Department of Geography, Rutgers, State University of New Jersey, Piscataway, NJ 08854, USA.